Coupling optogenetics and light-sheet microscopy to study signal transduction *in vivo*

Prameet Kaur[1], Timothy E. Saunders[2,3,4], Nicholas S. Tolwinski[1,3 *]

[1] Division of Science, Yale-NUS College, 12 College Ave West, #01- 201, Singapore 138610

[2] Mechanobiology Institute, National University of Singapore 117411, Singapore

[3] Department of Biological Sciences, National University of Singapore 117543, Singapore

[4] Institute of Molecular and Cell Biology, A*Star, Proteos 138673, Singapore

***** Correspondence: Nicholas.Tolwinski@yale-nus.edu.sg

Tel.: +65-6601-3092

Abstract (167 words)

Optogenetics allows precise, fast and reversible intervention in biological processes. Coupled with light-sheet microscopy, this approach allows unparalleled insight into the regulation of signaling pathways and cellular processes from a spatial and temporal perspective *in vivo*. To develop this method, we investigated the spatial and temporal regulation of canonical Wnt signaling during anterior-posterior patterning of the *Drosophila* embryonic epidermis. Cryptochrome C (Cry2) from *Arabidopsis Thaliana* was fused to mCherry fluorescent protein and *Drosophila* β–catenin to form an easy to visualize optogenetic switch. Blue light illumination caused reversible oligomerization of the fusion protein and inhibited downstream Wnt signaling *in vitro* and *in vivo*. Temporal inactivation of β–catenin showed that Wnt signaling is required not only for *Drosophila* patterning formation, but also for maintenance throughout development. By applying light-sheet microscopy to activate the pathway and then record subsequent behavior *in toto*, we show precise spatial regulation of Wnt signaling *in vivo*. We anticipate that this method will be easily extendable to other developmental signaling pathways and many other experimental systems.

Introduction

Dissections of signaling pathways and their downstream processes have centered on *in vitro* cell culture models and *in vivo* model organism studies using small molecule, knockdown and overexpression approaches. Although these approaches have been very useful, they do not lend themselves easily to the study of the spatial and temporal regulation of cell signaling pathways and cellular processes in the dynamic environment of a living organism. Normal genetic crosses using mutations and RNAi techniques are limited in their applications as they result in irreversible knockout or knockdown of a gene, which can be lethal or incomplete[1]. The recent discovery of optogenetic tools has provided a new and effective toolbox for spatial and temporal regulation of proteins in various *in vitro* and *in vivo* systems [2-5]. This is made possible by the rapid and reversible response of these proteins to light, such as the blue-light mediated activation of *Arabidopsis thaliana* cryptochrome 2 (Cry2)[6].

The application of optogenetic tools is only as good as the visualization approach that can be brought to bear. The latest advances in light-sheet microscopy facilitate high resolution optical sectioning and live imaging of embryos with low phototoxicity as compared to conventional laser confocal imaging[7]. Importantly, light-sheet microscopy enables selective activation of optogenetic insertions without significant out-of-plane effects. This contrasts with confocal activation, where optogenetic components above and below the focal plane (but inside the focal light cone) are activated as the system is typically highly light sensitive. In addition, new, stable fluorescent proteins allow imaging of various cellular processes at the same time[8]. Combining all three of these advances allowed us to develop a method for dissecting temporal and spatial regulation of Wnt signaling to address the key developmental signaling question of when is Wnt required.

The Wnt pathway is a highly conserved signal transduction pathway functioning in development and disease in many organisms[9]. In *Drosophila*, Wnt1 (Wingless or Wg) is a segment polarity gene that defines anterior-posterior patterning of the epidermis[10,11]. Canonical Wnt signaling is activated by inhibiting cellular β-catenin degradation (Armadillo or Arm in *Drosophila*). As β-catenin protein levels increase, it enters the nucleus where it regulates transcription of target genes by associating with the transcription factor TCF[12,13]. This basic signaling mechanism is widely conserved, and critical in embryogenesis, but whether β-catenin signaling is needed in a constant widespread manner, versus in a temporally and/or spatially restricted manner was not known, because the tools needed to address this question were lacking.

Here we describe our application of Cry2 technology to investigate the spatial and temporal regulation of β-catenin protein in the developing embryo. We established a system that allowed reversible inactivation of β-catenin through blue-light illumination coupled with live imaging in a second spectrum using light-sheet microscopy. We used this tool to determine the precise location and timing of β–catenin function during Wnt signaling and found that Wnt signaling must be maintained late in embryogenesis for normal patterning.

Results

Light-induced oligomerisation of β–catenin-Cry2-mCh modulates Wnt signaling in vitro

Blue light can induce oligomerization of *A. thaliana* Cry2 to form 'photobodies' in plant and mammalian cells through light induced binding to CIB[6,14]. This leads to sequestration and hence functional inactivation of the protein. We tested this mechanism by fusing the photolyase homology region (PHR) of Cry2 and mCherry to the C terminus of *Drosophila* β–catenin or Arm protein (Arm-Cry2-mCh). To determine if the Arm-Cry2-mCh construct was responsive to light, it was transfected into S2R+ Wnt responsive *Drosophila* cells. Distinct fluorescent puncta were observed with blue light illumination (Fig. 1A; full construct details in Supplementary Fig. 1). The puncta dispersed rapidly upon withdrawal of blue light (Fig. 1A).

We next investigated if inducible Arm-Cry2-mCh puncta formation functionally inactivated Arm activity. The effect of the Arm-Cry2-mCh construct on canonical Wnt signaling was determined by using a TOPFlash reporter assay, where the luciferase gene is attached downstream of multimerized TCF binding sites. Overexpression of Arm-Cry2-mCh in S2R+ cells in the absence of light significantly increased TOPflash activity relative to control transfected cultures (Fig. 1B). This activation was inhibited when transfected cells were illuminated with light. Hence, oligomerization of the Arm-Cry2-mCh construct upon illumination with light effectively blocked downstream Wnt signaling.

Having verified the responsiveness of the Arm-Cry2-mCh construct to blue light illumination and its ability to modulate Wnt signaling *in vitro*, we tested the oligomerization of this construct in *Drosophila* embryos. Expression in wild type embryos showed the cytoplasmic and diffuse localization of Arm as indicated by the mCh fluorescence (Fig. 1C,

Supplementary video 1). Upon blue light illumination, distinct fluorescent puncta were observed which dispersed upon withdrawal of blue light (Fig. 1C, Supplementary video 1). Re-illumination with blue light resulted in renewed oligomerization that was again reversed when blue light was withdrawn. These results show an *in vivo*, reversible, light-responsive aggregation of β–catenin during development of the *Drosophila* embryo.

Arm-Cry2-mCh can rescue patterning in arm^{XM19} mutant embryos

In order to establish the ability of the Arm-Cry2-mCh construct to function in place of endogenous Arm, we expressed it in an *arm^{XM19}* mutant background. We used *arm^{XM19}* mutants, because these lack the C terminus required for transcriptional transactivation but do not lose adhesion (Fig. 2A)[15]. Wild-type *Drosophila* embryos show an alternating pattern of naked cuticle and denticles[11]. When canonical Wnt signaling is turned off, all ventral epidermal cells produce denticles. The opposite is true when Wnt signaling is turned on ectopically; most cells do not make denticles causing the naked phenotype. Germline clones of *arm^{XM19}* were made in which the maternal and zygotic contribution of protein was removed[16], resulting in an embryonic phenotype identical to *wg* mutant embryos (Fig. 2B)[17]. In these embryos, we expressed Arm-Cry2-mCh and saw a rescue of the canonical signaling defect (Fig. 2B) where *arm^{XM19}* mutants with Arm-Cry2-mCh showed a nearly wild type denticle pattern as long as the embryos were kept in the dark (Fig. 2B). When exposed to light, we observed no rescue of the canonical signaling defect as embryos showed the null signaling phenotype (Fig. 2B). Taken together, these results suggest that the Arm-Cry2-mCh construct can effectively rescue canonical Wnt signaling in *arm^{XM19}* mutant embryos, and that this rescue can be blocked by exposure to light.

To confirm the Wnt dependence of the phenotype, we examined genes downstream of Wnt signaling using quantitative PCR. Expression of the embryonic Wnt target genes En and Wg was significantly decreased in Arm-Cry2-mCh expressing *arm*^{XM19} mutants exposed to light as contrasted with embryos kept in the dark both quantitatively (Fig. 2C), and qualitatively through immunostaining for En protein (Fig. 2D). In the absence of light, stripes of En protein were observed but these were lost with blue light illumination (Fig. 2D).

Next, we used light-sheet microscopy to live-image these embryos. *arm*^{XM19} mutants expressing the Arm-Cry2-mCh construct (as observed by luminescence upon excitation with the 561nm laser), showed normal embryonic development (Fig. 2E, Supplementary video 2A) similar to embryos expressing Arm-GFP (Supplementary video 2C). We next exposed these embryos to blue light and observed smaller embryos developing with a lawn of denticles (Fig. 2E, Supplementary video 2B), consistent with a loss of Wnt signaling. We catalogued a variety of other defects including defective head involution, incomplete germ band retraction, incomplete development of the intestines among other developmental phenotypes that will be described elsewhere (Fig. 2E, Supplementary video 2B).

Temporal regulation of Wnt signaling during development in arm^{XM19} *embryos*

The previous experiments established the efficacy of the Arm-Cry2-mCh transgene in embryos. We next performed a temporal experiment to answer the biological question of when Wnt signaling becomes activated during *Drosophila* embryonic development and if it is required for maintenance of segment polarity. Eggs were exposed to light at different developmental stages[18]. The phenotype with exposure to light at different stages was determined from cuticle preparations. Exposure to light from stages 1 to 11 showed a lawn of denticles similar to *wg* mutants (Fig. 3A). The lawn of denticles began getting broader when

light was applied at stage 12 (onset germband retraction) with some distance developing between the denticle bands. This distance increased with later exposure to light until the bands separated out from each other at light exposure at stage 14-15 (start of heart formation, and end of germ band retraction). The denticle bands showed defects even if β-catenin was inactivated by exposure to light at much later time points, close to larval hatching (embryonic stage 16-17, muscle twitching)[18]. This experiment showed that Wnt signaling is required not just for the early establishment of parasegments, but Wnt function must be maintained throughout embryonic development for patterning to function.

Spatial perturbation of Wnt signaling during development in arm^{XM19} embryos

We next wanted to test the spatial resolution of this approach using light sheet microscopy as a blue light source as well as a recorder for live imaging. Half of an embryo overexpressing the Arm-Cry2-mCh transgene was illuminated with blue light and the whole embryo imaged in the red channel. The region of the embryo with blue light illumination showed similar defects as in the earlier results with the unilluminated half remaining more wild-type (Fig. 3B, Supplementary Video 3, compare to Supplementary Video 2A and 2B), showing that combining light sheet imaging with spatial activation of Wnt signaling can be used to make and image mosaic embryos.

Arm-Cry2-mCh can rescue patterning in arm^{XM19}, gsk3 mutant embryos

The results above show how Arm-Cry2-mCh replaced endogenous Arm and restored normal patterning and most importantly was regulated by blue light. We next applied this optogenetic tool to a gain of function scenario where embryos were maternally and zygotically mutant for both *arm^{XM19}* and *gsk3*. *arm^{XM19}*, *gsk3* germline clones display an embryonic phenotype identical to *wg* mutant embryos as *arm* is genetically completely

epistatic to *gsk3* and showing that Gsk3's main embryonic role is to phosphorylate Arm (Fig. 4A)[17,19]. Expression of Arm-Cry2-mCh in these embryos restored Arm function and in the dark led to naked embryos (Fig. 4A), because *gsk3* mutants fail to degrade Arm resulting in Wnt hyper activation[15,19]. Despite the high levels of Arm protein in *gsk3* mutants, illumination led to a lawn of denticles suggesting that even with the high Arm levels light-induced Arm-Cry2-mCh aggregation could still block signaling (Fig. 4A). To confirm Wnt specificity, we performed qPCR measurement of the downstream Arm-responsive genes, En and Wg. These were significantly decreased in Arm-Cry2-mCh expressing, arm^{XM19}, *gsk3* mutants exposed to light as compared to embryos kept in the dark (Fig. 4B). Immunostaining for En protein showed that in the absence of light, En stripes were wider as compared to wild-type embryos (Fig. 2D), but these were lost upon blue light illumination (Fig. 4C).

We looked at these embryos through live imaging using light-sheet microscopy. arm^{XM19}, *gsk3* mutants expressing Arm-Cry2-mCh without blue light arrested during germ band retraction similar to *gsk3* mutants (Fig. 4D, Supplementary video 4A)[20]. When exposed to blue light, we observed a short embryo with a lawn of denticles (Fig. 4D, Supplementary video 4B). These embryos exhibited a variety of additional phenotypes without exposure to light including intestinal development and head involution defects, which were reversed by blue light illumination (Fig. 4D, Supplementary video 4B). We conclude that Arm-Cry2-mCh can replace Arm function completely under both normal and gain of function conditions.

Temporal and spatial regulation of Wnt signaling during development in arm^{XM19}, gsk3 embryos

We next asked what is the time dependence of Wnt signaling during development (Fig. 5A). Arm inactivation by exposure to light during earlier development stages (stage 1 to 11) produced a lawn of denticles similar to *wg* mutants (Fig. 5A). As Arm inactivation by light was delayed by stages, the lawn of denticles began getting broader with fewer denticles with later exposure to light till a naked phenotype with few denticles was observed even upon exposure to light at much later developmental stages (embryonic stage 14-17)[18]. This result again shows that Wnt signaling is required both for establishment and maintenance of patterning.

When these embryos were kept in the dark, we were able to reproduce an ectopic Wnt phenotype bringing up the possibility that we could make mosaic embryos with regions of inactive signaling in an epithelium of hyper-active Wnt. To explore the spatial function of Wnt signaling in these embryos, half of an embryo overexpressing the Arm-Cry2-mCh transgene was illuminated with blue light while the whole embryo was imaged in the red channel. The region of the embryo with blue light illumination showed similar defects as in the earlier results (Fig. 5B, Supplementary Video 5, compare to Supplementary Video 2A and 2B), while the un-illuminated region appeared to develop normally.

Light-responsive properties of Arm-Cry2-mCh can modulate Wnt signaling in HEK293

We have shown that Arm-Cry2-mCh functions in insect cells and in *Drosophila* embryos. We next tested if this construct could be applied to other experimental systems by looking at whether it could be used to modulate Wnt signaling in mammalian cells. We used HEK293 (Human embryonic kidney cells) stably transfected with the Wnt3a gene and TOPFlash vector (HEK293-Wnt3a-TOPFlash). Cells transfected with the construct showed fluorescent

puncta formation upon blue light illumination (Fig. 6A). The puncta dispersed rapidly upon withdrawal of blue light (Fig. 6A).

The effect of inducible Arm-Cry2-mCh clustering on Wnt signaling in mammalian cells was quantified using a TOPFlash reporter assay. Overexpression of Arm-Cry2-mCh plasmid in HEK293-Wnt3a-TOPFlash cells in the absence of light significantly increased TOPflash activity relative to control transfected cultures (Fig. 6B). This activation was inhibited when transfected cells were exposed to light. Our data suggest that oligomerization of the Arm-Cry2-mCh construct upon illumination with light could be applied to other experimental systems.

Discussion

Classical genetics tools allow tissue-specific manipulation of gene expression, but not precise temporal or spatial manipulation. For example, previous studies using temperature sensitive alleles and heat-shock induced expression were not precise due to the time it took to change the temperature of developing embryos[17,21-23]. Optogenetic tools can address this problem by allowing spatial and temporal regulation in a rapid, precise, and reversible manner[2,24,25]. Our study is the first study to combine optogenetics with light-sheet microscopy for noninvasive temporal and spatial control of cell signaling *in vivo*. Using these tools, we investigated the spatial and temporal regulation of β–catenin and Wnt signaling *in vivo* and *in vitro* proving the efficacy of this method. Wnt's role in segment polarity is well known[26,27], and we observed the same phenotypes by inactivating Wnt signaling during early stages of development (stage 1 to 11). But, we found that exposure to light at later stages in development also resulted in abnormal denticle patterning with loss of naked cuticle and closely packed denticle bands, emphasizing just how malleable cell fates can be and how late Wnt must act to maintain specific cell fates in epithelial cells[28].

Light-sheet microscopy allows blue-light induced oligomerization using the 488nm laser light and tracking of Arm fused to mCherry fluorescent protein using the 561nm laser light. Cry2 normally requires binding to CIB1, a basic helix-loop-helix (bHLH) protein upon photoexcitation by blue light[29], but Cry2 was shown to be sufficient to induce oligomerization and activation of the Wnt co-receptor, LRP6 without the need for CIB1[3]. We find that Cry2 oligomerization suffices to inactivate β–catenin signaling. We postulate that oligomerization prevents β–catenin from translocating to the nucleus, possibly due to the inaccessibility of the Armadillo repeat sequences to interact with the nuclear pore complex that mediates translocation to the nucleus[30].

Wnt signaling in segment polarity is well studied, but many additional functions have been observed[11]. Recently, Akiyoshi et al[31] reported that intestinal formation during embryo development was disrupted in embryos treated with ionomycin, an inhibitor of Wnt/β-catenin signaling. By coupling optogenetics with live imaging, we observed a similar defect in intestinal development in Arm-Cry2-mCh expressing *arm*^{XM19} mutant embryos. Our experiment with spatial activation of Arm-Cry2-mCh in only half the embryo, also confirmed these findings. Taken together, we see the application of optogenetics with light-sheet microscopy will allow the exploration of many more Wnt pathway effects.

Our optogenetics approach is a non-invasive and versatile tool that allows for manipulation as well as live tracking of protein activity to interrogate complex phenotypes *in vivo*[32]. We foresee applying this tool to cell culture, organoid studies, vertebrate development in zebrafish, and many other systems. It provides an alternative to small molecule studies which can only be performed on druggable targets. We have made a human β–catenin-Cry2 version that functions similarly, and are proceeding to test the general applicability to other signaling pathways such as Ras.

Materials and Methods

Transgenes and GAL4 driver lines

Two ubiquitous drivers were used for expression of transgenes: the weaker armadillo-GAL4 and the stronger daughterless-GAL4[33]. The Arm-Cry2-mCh constructs were made using the MultiSite Gateway® Pro 2.0 cloning kit (Invitrogen). Full-length Armadillo was amplified from *Drosophila* embryo cDNA with *att*B1 and *att*B5r-flanked sites. This PCR product was recombined into pDONR P1-P5r vector. The Cry2-mCh was amplified from pCRY2PHR-mCherryN1 which was a gift from Chandra Tucker (Addgene plasmid # 26866)[6]. *att*B5 and *att*B2 sites were added to the Cry2-mCh PCR product and recombined into pDONR P5-P2 vector. Both pDONR vectors with Armadillo and Cry2-mCh insert were recombined by Gateway cloning (Invitrogen) into pUASg.attB with COOH-terminal 3XHA tag (A kind gift from J. Bischof and K. Basler, Zurich)[34] to obtain the Arm-Cry2-mCh transgene for expression in *Drosophila*. Transgenes were injected into attP2 (Strain #8622) P[CaryP]attP2 68A4 by BestGene Inc. (California)[35]. For constitutive expression in S2R+ cells, the pDONR vectors were recombined into the Gateway destination vector, pAW (Drosophila Gateway® Vector collection, Carnegie Institution). EGFP-tagged protein lines were derived using the *Minos* mediated integration cassette (MiMIC) methodology described by Nagarkar-Jaiswal et al.[36,37] and the Arm MiMIC line was obtained from the Bloomington Drosophila Stock Center (BDSC).

Crosses and expression of UAS constructs

The dominant female sterile technique was used to generate maternally mutant eggs [16]. Please see Flybase for details on mutants used (flybase.bio.indiana.edu). Mutants used: $arm^{XM19}$and $zw3^{M11\text{-}1}$[15]. For mis-expression experiments, the ArmGAL4 2nd chromosome was used. All X-chromosome mutants use FRT 101.

The following crosses were conducted:

1. *arm*^{XM19} FRT101/ovoD1 FRT101; Arm-Gal4 x w; UAS-Arm-Cry2-mCh
2. *arm*^{XM19} *zw3*$^{M11-1}$ FRT101/ovoD1 FRT101; Arm-Gal4 x w; UAS-Arm-Cry2-mCh

Light-sheet microscopy

Living imaging of *Drosophila* embryos was carried out on the light-sheet Z.1 fluorescence microscope (Carl Zeiss, Germany) with W Plan-Apochromat 20×/1.0 UV-VIS detection objective (Carl Zeiss, Germany). Embryos were imaged using dual-side illumination by a light-sheet modulated into a pivot scan mode, with excitation laser lines 488 nm and 561 nm with emission filter BP505-545 and LP585 respectively. Image acquisition was done every 2.5 min in Z-stack mode. All SPIM data was saved in the LSM format and processed using ZEN software (Zeiss). Maximum intensity projections were generated from each z-stack file [38].

Antibodies and Immunofluorescence

Embryos were fixed with heptane/4% formaldehyde in phosphate buffer (0.1M NaPO4 pH 7.4)[39]. The antibodies used were: anti-Engrailed (mAb 4D9, Developmental Studies Hybridoma Bank developed under the auspices of the NICHD and maintained by The University of Iowa, Department of Biological Sciences, Iowa City, IA 52242). Staining, detection and image processing as described in Colosimo and Tolwinski[40].

Live-cell imaging.

Time-lapse microscopy of activated Cry2 fusions in S2R+ and HEK 293T cells was performed using a Zeiss Axioimager (Zeiss). Clustering visualization was carried out at room

temperature. Blue light exposure and mCherry imaging were performed simultaneous by imaging in both 488-nm and 561-nm laser channels.

TOPflash assay

TOPflash luciferase assays (TCF/LEF reporter assays) were performed to assess the effect of light on canonical Wnt-signalling in cells transfected with the Arm-Cry2-mCh plasmid. S2R+ cells were co-transfected with TOPflash[41], Renilla luciferase-Pol III and the Arm-Cry2-mCh plasmid using lipofectamine 3000 (ThermoFisher Scientific) according to the manufacturer's instructions. Cell lysates were prepared 24 hours after transfection and luciferase activity was measured using the Dual-Luciferase Reporter Assay System (Promega) according to the manufacturer's instructions. The relative TOPflash luciferase activity was measured using the ratio of firefly/renilla luciferase activity and the data was presented as mean ± SD.

RNA Extraction, cDNA Synthesis and qPCR

Mixed stage embryos, 0 to 16 hours after deposition, were exposed to light or no light for 6 hours, dechorionated in bleach, washed in water and collected. Total RNA was extracted for each treatment using the RNeasy Mini Kit (Qiagen) as per the manufacturer’s protocol. Total RNA concentration and purity was measured using the Cytation 3 Cell Imaging Multi-Mode Reader (BioTek). One µg of total RNA was reverse transcribed in a 20µl reaction volume using the QuantiTect reverse transcription kit (Qiagen) according to the manufacturer's protocol. Gene specific primer sequences were obtained from Fly Primer Bank[42]. Quantification of mRNA was performed using SYBR® Green Assay (Thermo Fisher Scientific) on the PikoReal™ Real-Time PCR System (Thermo Fisher Scientific) and a PCR product dissociation curve was generated to ensure specificity of amplification. For expression analysis, the mRNA data were normalized to the endogenous control, RPL32, followed by calibration to cultures not exposed to light using relative quantification ($2^{-\Delta\Delta CT}$).

Results were generated from 3 technical replicates for each mRNA. The average relative expression ± standard deviation (SD) was determined and two sample t-test was carried out to determine statistical significance.

Acknowledgments

We thank Yale-NUS students, Le Van Canh, Hyung-Seok Kim and Xiao Linfan for their help. This work was supported by an Academic Research Fund (AcRF) grant (MOE2014-T2-2-039) of the Ministry of Education, Singapore to NST. TES was supported by a National Research Foundation NRF Fellowship (NRF2012NRF-NRFF001-094).

Figures Legends

Figure 1. Light-induced clustering of Arm-Cry2-mCh modulates the Wnt/β-catenin pathway in *Drosophila*. (A) Arm-Cry2-mCh puncta formation in S2R+ cells in response to 488-nm laser light, as well as dissociation after light withdrawal. (B) S2R+ cells transfected with pAct-Arm-Cry2-mCh plasmid and the TOPFlash luciferase reporter showed reduced TOPFlash activity after 16hr exposure to light. Graph is representative of three independent experiments and the average of three replicates (mean ± SD). Statistical significance relative to control samples was determined using the Student's t-test. **$p<0.01$ relative to control, $^{\#\#}p<0.01$. (C) Arm-Cry2-mCh puncta formation in *Drosophila* embryos overexpressing Arm-Cry2-mCh in a wild-type background upon exposure to 488-nm laser light. Puncta formation observed during illumination was reversible and oligomerization could be induced repeatedly.

Figure 2. Arm-Cry2-mCh rescue of arm^{XM19} mutants is reversible with blue light. (A) Structure of arm^{XM19} truncated protein (adapted from Tolwinski and Weischaus[15]). The N-terminus of Arm is required for transactivation, phosphorylation-based and proteasome-mediated degradation, and α-catenin binding. The central repeats contain the binding sites for most of Arm's binding partners, such as APC, TCF, Cadherin, and Axin. The C-terminus is required for Cby and Teashirt binding and transactivation. arm^{XM19} lacks the entire C-terminus. (B) Cuticle preparations of arm^{XM19} mutant (germline clone, GLC) embryo with entire cuticle covered with denticles, arm^{XM19} GLC expressing Arm-Cry2-mCh without light was rescued to a wild-type cuticle, arm^{XM19} GLC expressing Arm-Cry2-mCh with illumination showed defective wg signaling with cuticle covered with denticles. (C) Quantitative expression of genes downstream of Wg signaling in Arm-Cry2-mCh overexpressing arm^{XM19} mutants. Embryos exposed to light showed reduced *En* and *Wg* gene

expression. Graph is representative of three independent experiments and the average of three replicates (mean ± SD). Statistical significance relative to control samples was determined using the Student's t-test. *p<0.05, **p<0.01. (D) En antibody staining in Arm-Cry2-mCh overexpressing *arm*^{XM19} mutant embryos illuminated or not illuminated with light. En stripes as in wild-type embryos were observed in embryos not illuminated with light whereas embryos illuminated with light showed only small patches of En expression. (E) Stills from live imaging movies of Arm-Cry2-mCh overexpressing *arm*^{XM19} mutants. Embryos not subjected to light showed diffused localization of Arm-Cry2-mCh (inset) as compared to embryos subjected to light (inset). Embryos not subjected to light showed normal development whereas embryos subjected to light showed various developmental defects.

Figure 3. Temporal and spatial inactivation of Arm-Cry2-mCh in *arm*^{XM19} mutant embryos overexpressing Arm-Cry2-mCh. (A) *arm*^{XM19} mutant embryos overexpressing Arm-Cry2-mCh were collected and exposed to light at various developmental stages. Cuticle preparations were carried out after light exposure. Exposure to light earlier (stage 1 to 11) during development resulted in a *wg* mutant phenotype. The denticle patterning began spreading out thereafter until stage 15 after which distinct denticle bands merging with each other could be observed till stage 17. (B) Spatial perturbation of Wnt signaling in Arm-Cry2-mCh overexpressing *arm*^{XM19} mutant embryos. The right half of the embryo was illuminated with 488nm laser light and the whole embryo was imaged simultaneously using light sheet microscopy. The right side of the embryo (with blue light illumination) showed distinct clustering, developmental defects as well as more closely packed denticle bands.

Figure 4. Arm-Cry2-mCh rescue of *arm*^{XM19}, *gsk3* mutants is reversible with blue light. (A) Cuticle preparations of *arm*^{XM19}, *gsk3* GLC embryo with entire cuticle covered with denticles,

arm^{XM19}, *gsk3* GLC expressing Arm-Cry2-mCh without light was rescued to a naked cuticle, *arm*^{XM19}, *gsk3* GLC expressing Arm-Cry2-mCh with illumination showed defective wg signaling with cuticle covered with denticles. (B) Quantitative expression of genes downstream of Wg signaling in Arm-Cry2-mCh overexpressing *arm*^{XM19}, *gsk3* mutants. Embryos exposed to light showed reduced *En* and *Wg* gene expression. Graph is representative of three independent experiments and the average of three replicates (mean ± SD). Statistical significance relative to control samples was determined using the Student's t-test. $^{**}p<0.01$. (C) En antibody staining in Arm-Cry2-mCh overexpressing *arm*^{XM19}, *gsk3* mutant embryos illuminated or not illuminated with light. Widened stripes of En protein were observed in embryos not illuminated with light as compared to wild-type embryos whereas embryos illuminated with light showed only small patches of En expression. (D) Stills from live imaging movies of Arm-Cry2-mCh overexpressing *arm*^{XM19}, *gsk3* mutants. Embryos not subjected to light showed incomplete germ band retraction whereas embryos subjected to light showed a smaller embryo, incomplete germ band retraction and defective head development.

Figure 5. Temporal and spatial inactivation of Arm-Cry2-mCh in *arm*^{XM19}, *gsk3* mutant embryos overexpressing Arm-Cry2-mCh. (A) *arm*^{XM19}, *gsk3* mutant embryos overexpressing Arm-Cry2-mCh were collected and exposed to light at various developmental stages. Cuticle preparations were carried out after light exposure. Exposure to light earlier (stage 1 to 11) during development resulted in a *wg* mutant phenotype. The denticle patterning began decreasing thereafter with fewer denticles observed till stage 17. (B) Spatial perturbation of Wnt signaling in Arm-Cry2-mCh overexpressing *arm*^{XM19}, *gsk3* mutant embryos. The right half of the embryo was illuminated with 488nm laser light and the whole embryo was imaged simultaneously using light sheet microscopy. The right side of the embryo (with blue light

illumination) showed distinct developmental defects as well as more denticles than the left half.

Figure 6. Light-induced clustering of Arm-Cry2-mCh modulates the Wnt/β-catenin pathway in mammalian cells. (A) Arm-Cry2-mCh puncta formation in HEK293-Wnt3a-TOPFlash cells in response to 488-nm laser light, as well as dissociation after light withdrawal. (B) HEK 293-Wnt3a-TOPFlash cells transfected with pAct-Arm-Cry2-mCh plasmid and the TOPFlash luciferase reporter showed reduced TOPFlash activity after exposure to light. Graph is representative of three independent experiments and the average of three replicates (mean ± SD). Statistical significance relative to control samples was determined using the Student's t-test. $^{**}p<0.01$ relative to control, $^{\#\#}p<0.01$.

Supplementary Videos Legends

Supplementary Video 1. Arm-Cry2-mCh puncta formation in *Drosophila* embryos overexpressing Arm-Cry2-mCh in a wild-type background upon exposure to 488-nm laser light. Puncta formation observed during illumination was reversible and oligomerization could be induced repeatedly.

Supplementary Video 2A. Arm-Cry2-mCh overexpressing arm^{XM19} mutant embryos not exposed to light showed diffuse localization of Arm-Cry2-mCh and normal embryonic development.

Supplementary Video 2B. Arm-Cry2-mCh overexpressing arm^{XM19} mutant embryos exposed to 488nm light showed distinct puncta formation of Arm-Cry2-mCh and various developmental defects as compared to embryos not exposed to light.

Supplementary Video 2C. Embryos expressing Arm-EGFP showed normal embryonic development.

Supplementary Video 3. Spatial perturbation of Wnt signaling in Arm-Cry2-mCh overexpressing arm^{XM19} mutant embryos. The right half of the embryo was illuminated with 488nm laser light and the whole embryo was imaged simultaneously in the red channel. The right side of the embryo (with blue light illumination) showed distinct clustering and developmental defects.

Supplementary Video 4A. Arm-Cry2-mCh overexpressing *arm*^{XM19}, *gsk3* mutant embryos not exposed to blue light showed diffuse localization of Arm-Cry2-mCh and incomplete germ band retraction.

Supplementary Video 4B. Arm-Cry2-mCh overexpressing *arm*^{XM19}, *gsk3* mutant embryos exposed to 488nm light showed distinct puncta formation of Arm-Cry2-mCh, a small embryo, incomplete germ band retraction and defective head development.

Supplementary Video 5. Spatial perturbation of Wnt signaling in Arm-Cry2-mCh overexpressing *arm*^{XM19}, *gsk3* mutant embryos. The right half of the embryo was illuminated with 488nm laser light and the whole embryo was imaged simultaneously in the red channel. The right side of the embryo (with blue light illumination) showed distinct clustering and developmental defects.

References

1 Doupe, D. P. & Perrimon, N. Visualizing and manipulating temporal signaling dynamics with fluorescence-based tools. *Sci Signal* **7**, re1, doi:10.1126/scisignal.2005077 (2014).

2 Aravanis, A. M. *et al.* An optical neural interface: in vivo control of rodent motor cortex with integrated fiberoptic and optogenetic technology. *J Neural Eng* **4**, S143-156, doi:10.1088/1741-2560/4/3/S02 (2007).

3 Bugaj, L. J., Choksi, A. T., Mesuda, C. K., Kane, R. S. & Schaffer, D. V. Optogenetic protein clustering and signaling activation in mammalian cells. *Nat Methods* **10**, 249-252, doi:10.1038/nmeth.2360 (2013).

4 Liu, H., Gomez, G., Lin, S., Lin, S. & Lin, C. Optogenetic control of transcription in zebrafish. *PLoS One* **7**, e50738, doi:10.1371/journal.pone.0050738 (2012).

5 Konermann, S. *et al.* Optical control of mammalian endogenous transcription and epigenetic states. *Nature* **500**, 472-476, doi:10.1038/nature12466 (2013).

6 Kennedy, M. J. *et al.* Rapid blue-light-mediated induction of protein interactions in living cells. *Nat Methods* **7**, 973-975, doi:10.1038/nmeth.1524 (2010).

7 Huisken, J. & Stainier, D. Y. Selective plane illumination microscopy techniques in developmental biology. *Development* **136**, 1963-1975, doi:10.1242/dev.022426 (2009).

8 Chudakov, D. M., Matz, M. V., Lukyanov, S. & Lukyanov, K. A. Fluorescent proteins and their applications in imaging living cells and tissues. *Physiol Rev* **90**, 1103-1163, doi:10.1152/physrev.00038.2009 (2010).

9 Clevers, H. Wnt/beta-catenin signaling in development and disease. *Cell* **127**, 469-480, doi:10.1016/j.cell.2006.10.018 (2006).

10 Wodarz, A. & Nusse, R. Mechanisms of Wnt signaling in development. *Annu Rev Cell Dev Biol* **14**, 59-88 (1998).

11 Swarup, S. & Verheyen, E. M. Wnt/Wingless signaling in Drosophila. *Cold Spring Harb Perspect Biol* **4**, doi:10.1101/cshperspect.a007930 (2012).

12 Stadeli, R., Hoffmans, R. & Basler, K. Transcription under the control of nuclear Arm/beta-catenin. *Curr Biol* **16**, R378-385, doi:10.1016/j.cub.2006.04.019 (2006).

13 Mosimann, C., Hausmann, G. & Basler, K. Beta-catenin hits chromatin: regulation of Wnt target gene activation. *Nat Rev Mol Cell Biol* **10**, 276-286, doi:10.1038/nrm2654 (2009).

14 Mas, P., Devlin, P. F., Panda, S. & Kay, S. A. Functional interaction of phytochrome B and cryptochrome 2. *Nature* **408**, 207-211, doi:10.1038/35041583 (2000).

15 Tolwinski, N. S. & Wieschaus, E. A nuclear function for armadillo/beta-catenin. *PLoS Biol* **2**, E95 (2004).

16 Chou, T. B. & Perrimon, N. Use of a yeast site-specific recombinase to produce female germline chimeras in Drosophila. *Genetics* **131**, 643-653 (1992).

17 Peifer, M. & Wieschaus, E. The segment polarity gene armadillo encodes a functionally modular protein that is the Drosophila homolog of human plakoglobin. *Cell* **63**, 1167-1176 (1990).

18 Hartenstein, V. *Atlas of Drosophila development*. (Cold Spring Harbor Laboratory Press, 1993).

19 Siegfried, E., Wilder, E. L. & Perrimon, N. Components of wingless signalling in Drosophila. *Nature* **367**, 76-80 (1994).

20 Siegfried, E., Chou, T. B. & Perrimon, N. wingless signaling acts through zeste-white 3, the Drosophila homolog of glycogen synthase kinase-3, to regulate engrailed and establish cell fate. *Cell* **71**, 1167-1179 (1992).

21 DiNardo, S., Sher, E., Heemskerk-Jongens, J., Kassis, J. A. & O'Farrell, P. H. Two-tiered regulation of spatially patterned engrailed gene expression during Drosophila embryogenesis. *Nature* **332**, 604-609, doi:10.1038/332604a0 (1988).

22 Noordermeer, J., Johnston, P., Rijsewijk, F., Nusse, R. & Lawrence, P. A. The consequences of ubiquitous expression of the wingless gene in the Drosophila embryo. *Development* **116**, 711-719 (1992).
23 Bejsovec, A. & Martinez Arias, A. Roles of wingless in patterning the larval epidermis of Drosophila. *Development* **113**, 471-485 (1991).
24 Galvan, A., Hu, X., Smith, Y. & Wichmann, T. In vivo optogenetic control of striatal and thalamic neurons in non-human primates. *PLoS One* **7**, e50808, doi:10.1371/journal.pone.0050808 (2012).
25 Jia, Z. *et al.* Stimulating cardiac muscle by light: cardiac optogenetics by cell delivery. *Circ Arrhythm Electrophysiol* **4**, 753-760, doi:10.1161/CIRCEP.111.964247 (2011).
26 Willert, K. & Nusse, R. Beta-catenin: a key mediator of Wnt signaling. *Curr Opin Genet Dev* **8**, 95-102, doi:S0959-437X(98)80068-3 [pii] (1998).
27 Klingensmith, J. & Nusse, R. Signaling by wingless in Drosophila. *Dev Biol* **166**, 396-414, doi:S0012-1606(84)71325-X [pii]10.1006/dbio.1994.1325 (1994).
28 Munoz Descalzo, S. & Martinez Arias, A. The structure of Wntch signalling and the resolution of transition states in development. *Semin Cell Dev Biol* **23**, 443-449, doi:10.1016/j.semcdb.2012.01.012 (2012).
29 Liu, H. *et al.* Photoexcited CRY2 interacts with CIB1 to regulate transcription and floral initiation in Arabidopsis. *Science* **322**, 1535-1539, doi:10.1126/science.1163927 (2008).
30 Sharma, M., Jamieson, C., Johnson, M., Molloy, M. P. & Henderson, B. R. Specific armadillo repeat sequences facilitate beta-catenin nuclear transport in live cells via direct binding to nucleoporins Nup62, Nup153, and RanBP2/Nup358. *J Biol Chem* **287**, 819-831, doi:10.1074/jbc.M111.299099 (2012).
31 Akiyoshi, R., Kaneuch, T., Aigaki, T. & Suzuki, H. Bioluminescence imaging to track real-time armadillo promoter activity in live Drosophila embryos. *Anal Bioanal Chem* **406**, 5703-5713, doi:10.1007/s00216-014-8000-8 (2014).
32 Shin, Y. *et al.* Spatiotemporal Control of Intracellular Phase Transitions Using Light-Activated optoDroplets. *Cell* **168**, 159-171 e114, doi:10.1016/j.cell.2016.11.054 (2017).
33 Brand, A. H. & Perrimon, N. Targeted gene expression as a means of altering cell fates and generating dominant phenotypes. *Development* **118**, 401-415 (1993).
34 Bischof, J. *et al.* A versatile platform for creating a comprehensive UAS-ORFeome library in Drosophila. *Development* **140**, 2434-2442, doi:10.1242/dev.088757 (2013).
35 Groth, A. C., Fish, M., Nusse, R. & Calos, M. P. Construction of transgenic Drosophila by using the site-specific integrase from phage phiC31. *Genetics* **166**, 1775-1782 (2004).
36 Nagarkar-Jaiswal, S. *et al.* A genetic toolkit for tagging intronic MiMIC containing genes. *Elife* **4**, doi:10.7554/eLife.08469 (2015).
37 Venken, K. J. *et al.* MiMIC: a highly versatile transposon insertion resource for engineering Drosophila melanogaster genes. *Nat Methods* **8**, 737-743 (2011).
38 Novak, D., Kucharova, A., Ovecka, M., Komis, G. & Samaj, J. Developmental Nuclear Localization and Quantification of GFP-Tagged EB1c in Arabidopsis Root Using Light-Sheet Microscopy. *Front Plant Sci* **6**, 1187, doi:10.3389/fpls.2015.01187 (2015).
39 Tolwinski, N. S. & Wieschaus, E. Armadillo nuclear import is regulated by cytoplasmic anchor Axin and nuclear anchor dTCF/Pan. *Development* **128**, 2107-2117 (2001).
40 Colosimo, P. F. & Tolwinski, N. S. Wnt, Hedgehog and junctional Armadillo/beta-catenin establish planar polarity in the Drosophila embryo. *PLoS ONE* **1**, e9, doi:10.1371/journal.pone.0000009 (2006).
41 van de Wetering, M. *et al.* Armadillo coactivates transcription driven by the product of the Drosophila segment polarity gene dTCF. *Cell* **88**, 789-799 (1997).
42 Hu, Y. *et al.* FlyPrimerBank: an online database for Drosophila melanogaster gene expression analysis and knockdown evaluation of RNAi reagents. *G3 (Bethesda)* **3**, 1607-1616, doi:10.1534/g3.113.007021 (2013).

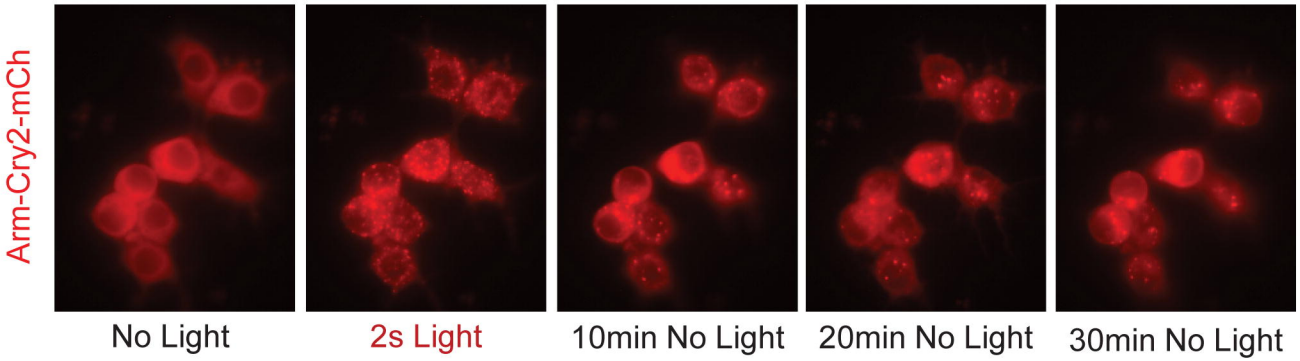
Arm-Cry2-mCh
No Light
2s Light
10min No Light
20min No Light
30min No Light

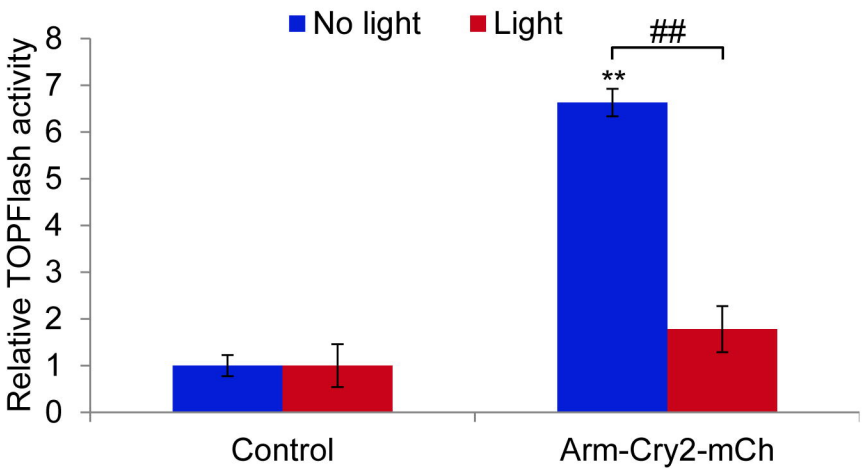
No light
Light
##
**
Relative TOPFlash activity
0
1
2
3
4
5
6
7
8
Control
Arm-Cry2-mCh

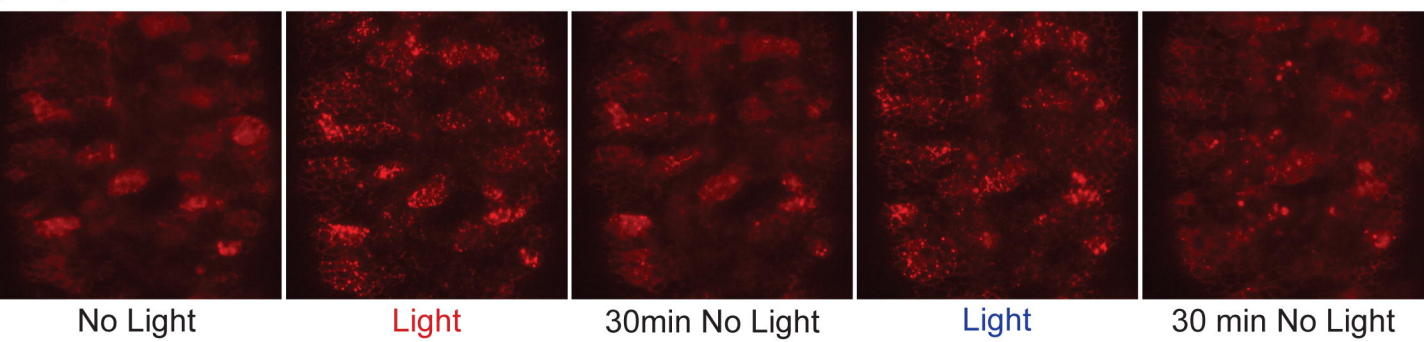
No Light
Light
30min No Light
Light
30 min No Light

2A

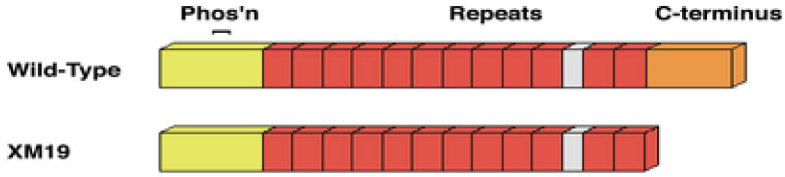
Phos'n
Repeats
C-terminus
Wild-Type
XM19

2B

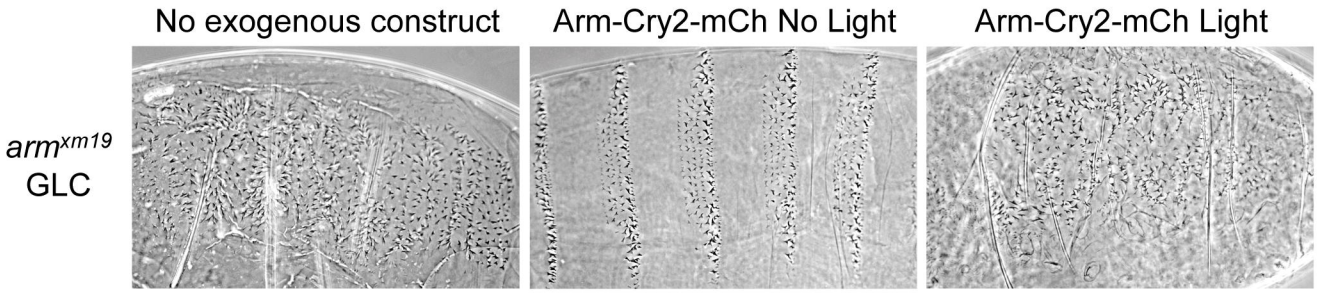
No exogenous construct
Arm-Cry2-mCh No Light
Arm-Cry2-mCh Light
armxm19
GLC

2C

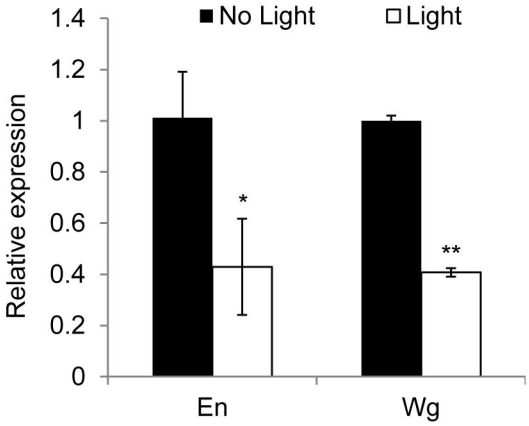
No Light
Light
Relative expression
1.4
1.2
1
0.8
0.6
0.4
0.2
0
*
**
En
Wg

2D

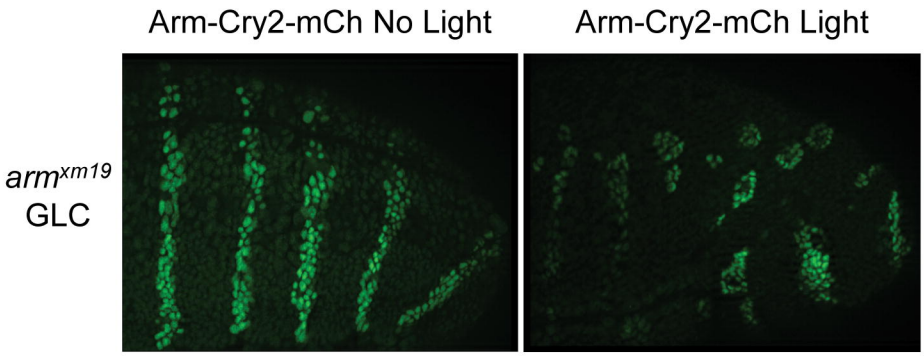
Arm-Cry2-mCh No Light
Arm-Cry2-mCh Light
armxm19
GLC

2E

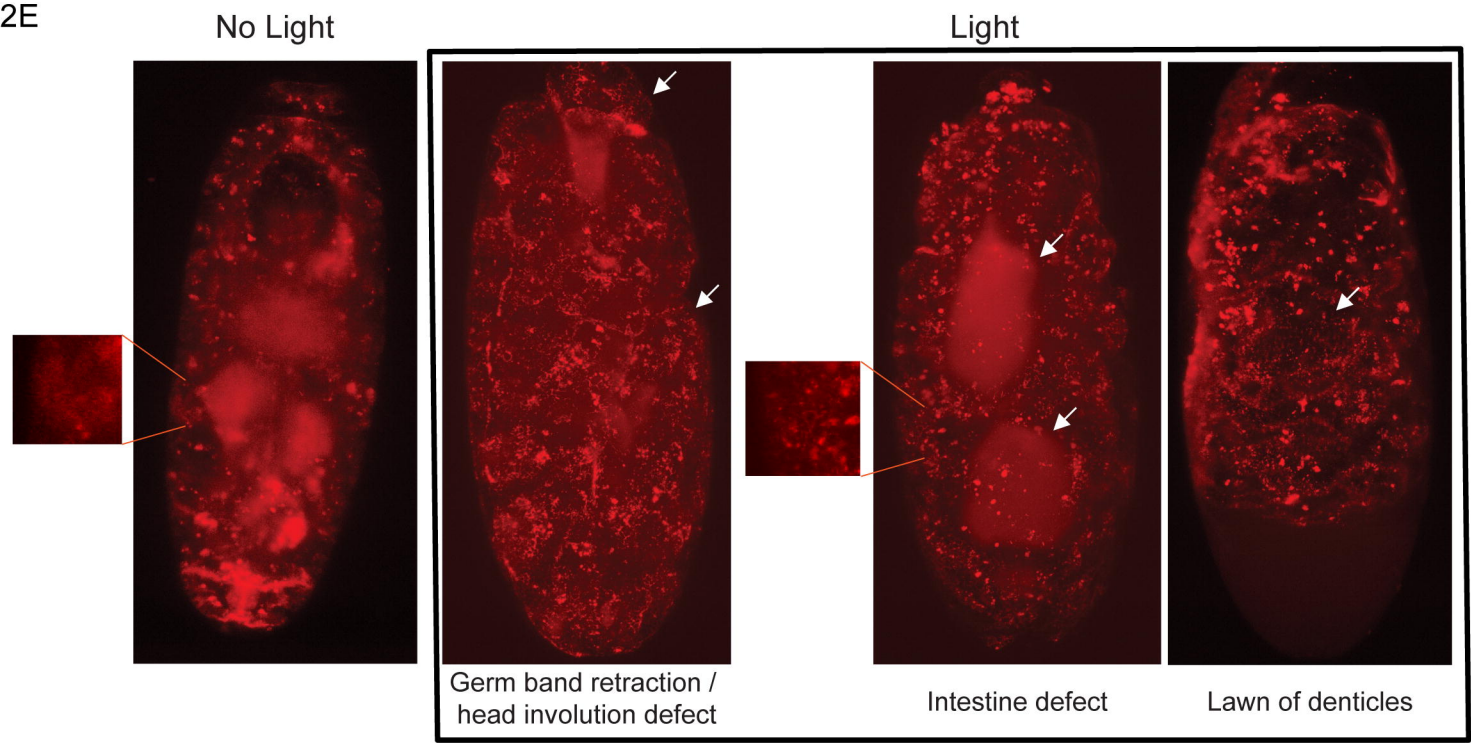
No Light
Light
Germ band retraction /
head involution defect
Intestine defect
Lawn of denticles

3A

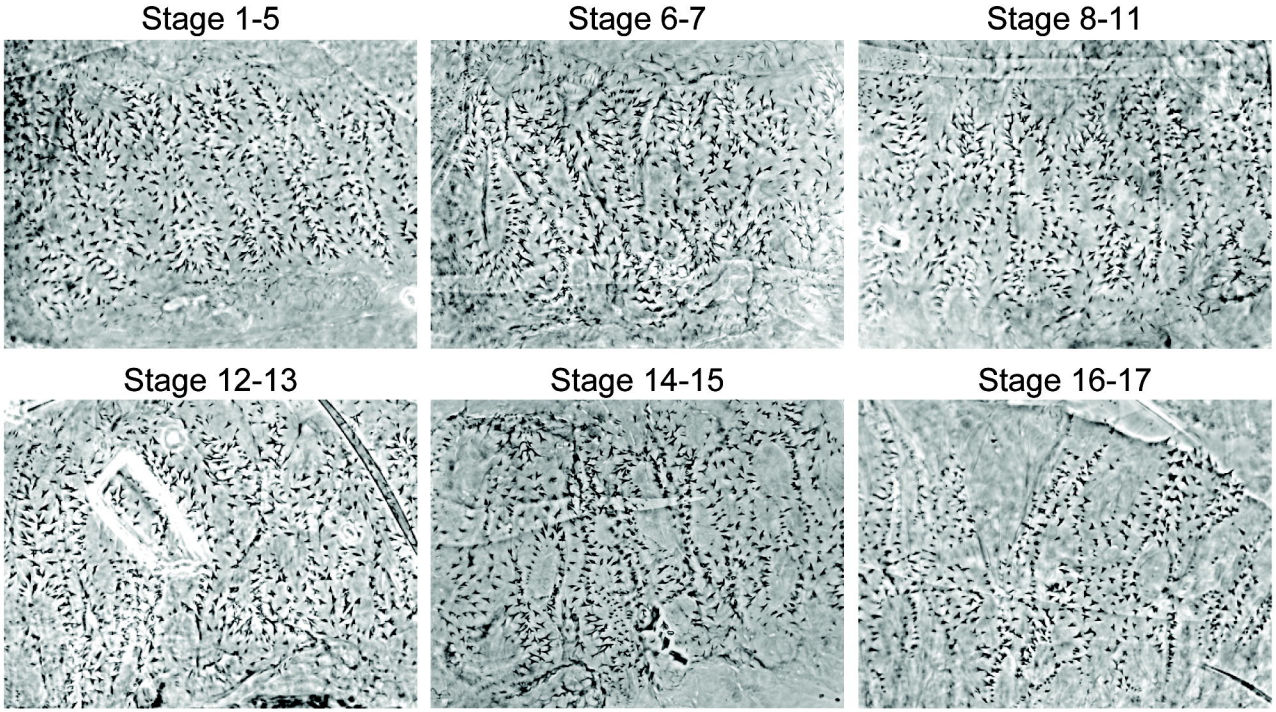

3B

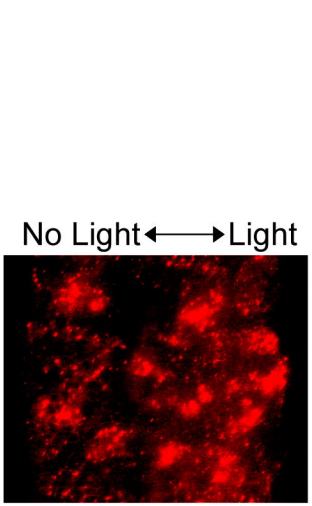

clustering

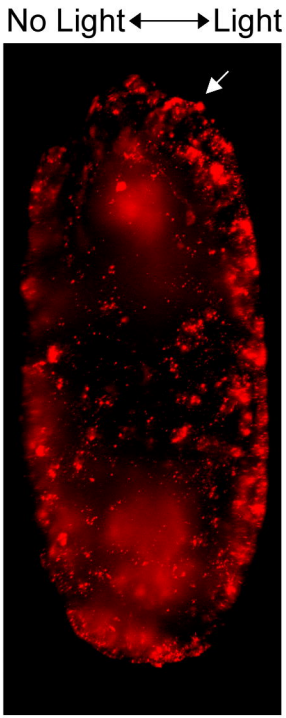

head involution defect

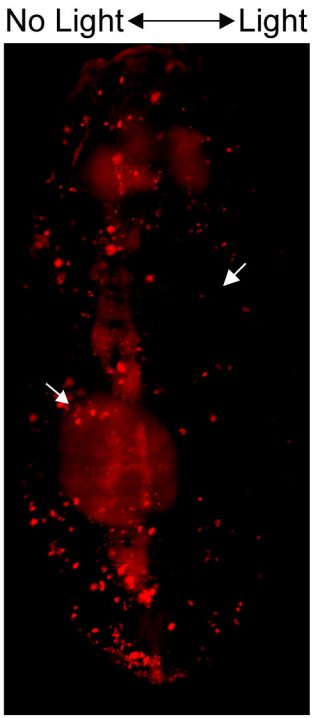

Intestine defect

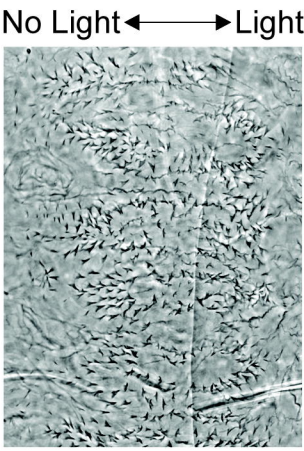

4A

No exogenous construct | Arm-Cry2-mCh No Light | Arm-Cry2-mCh Light

arm^{xm19},*gsk3* GLC

4B

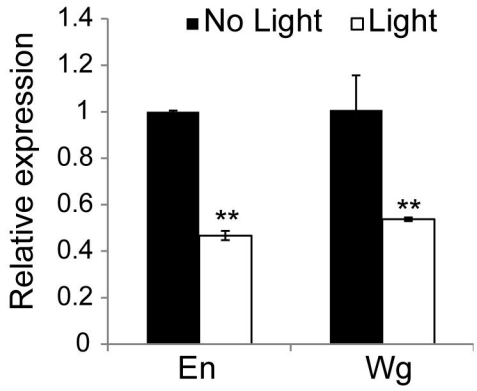

4C

Arm-Cry2-mCh No Light | Arm-Cry2-mCh Light

arm^{xm19},*gsk3* GLC

4D

No Light | Light

Germ band retraction defect | Head involution defect | Intestine defect | Germ band retraction / head involution defect | Intestine defect

5A

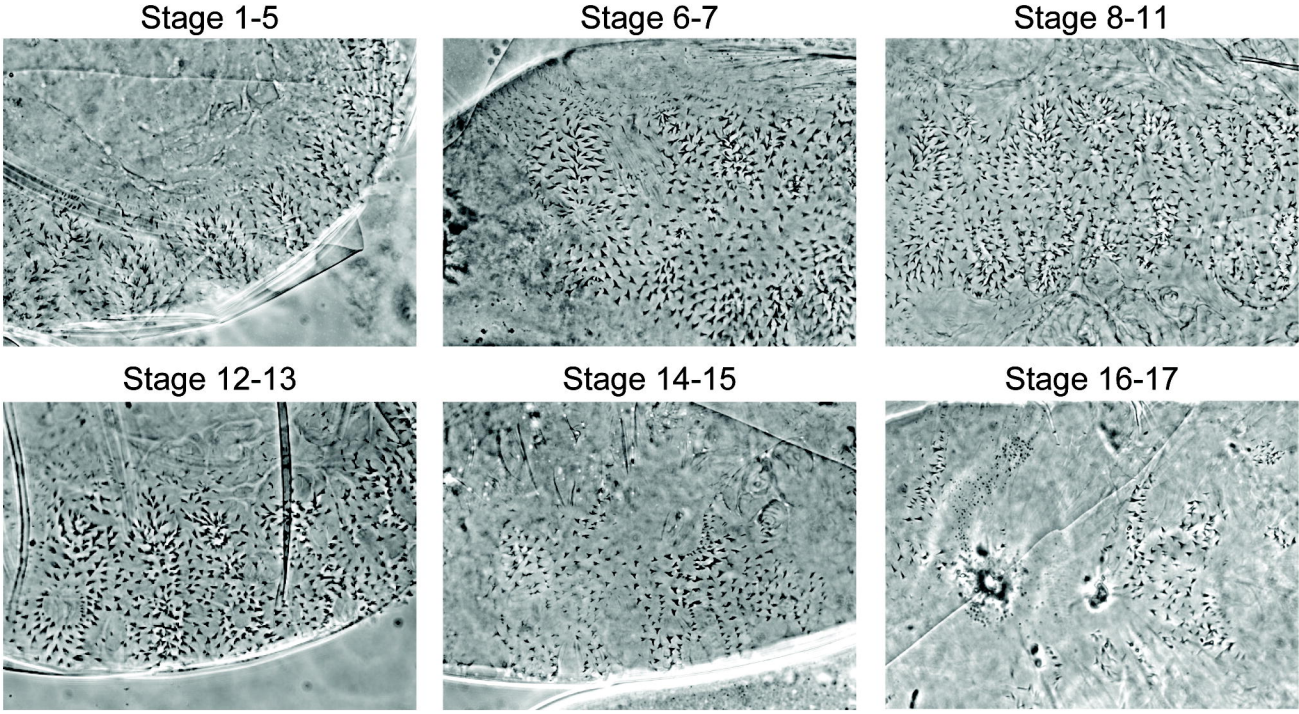
Stage 1-5
Stage 6-7
Stage 8-11
Stage 12-13
Stage 14-15
Stage 16-17

5B

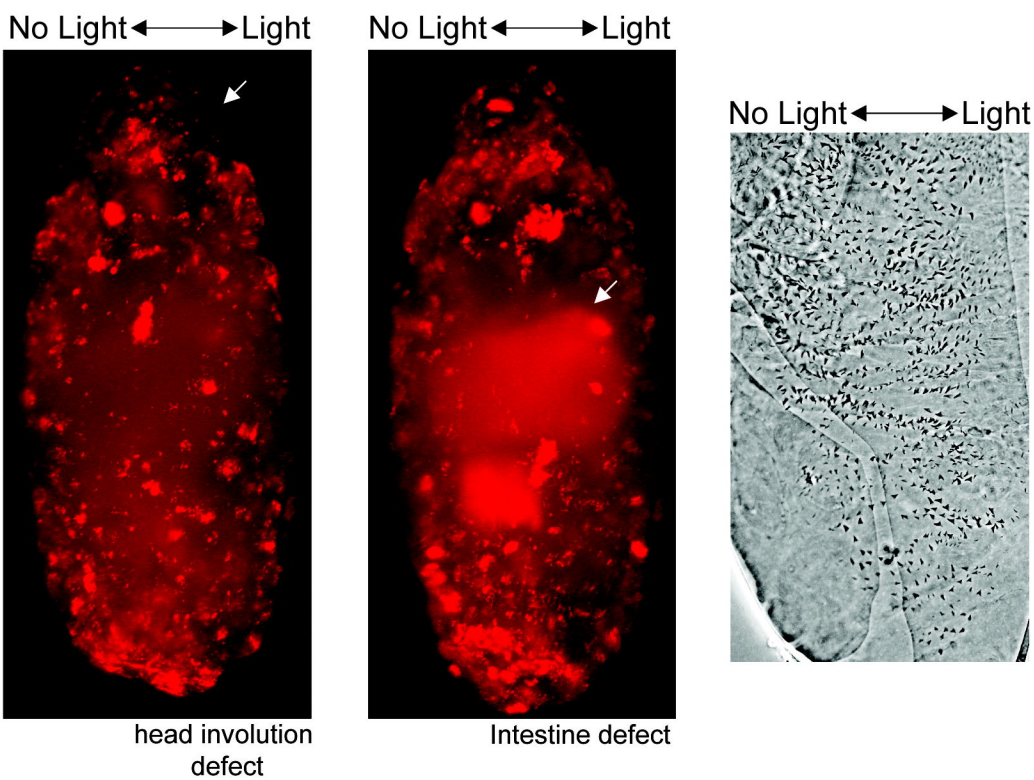
No Light ◄——► Light
No Light ◄——► Light
No Light ◄——► Light
head involution defect
Intestine defect

6A

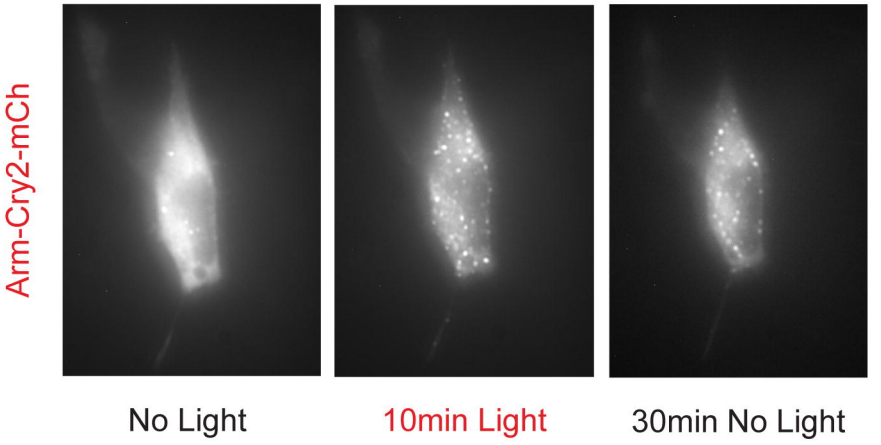
Arm-Cry2-mCh
No Light
10min Light
30min No Light

6B

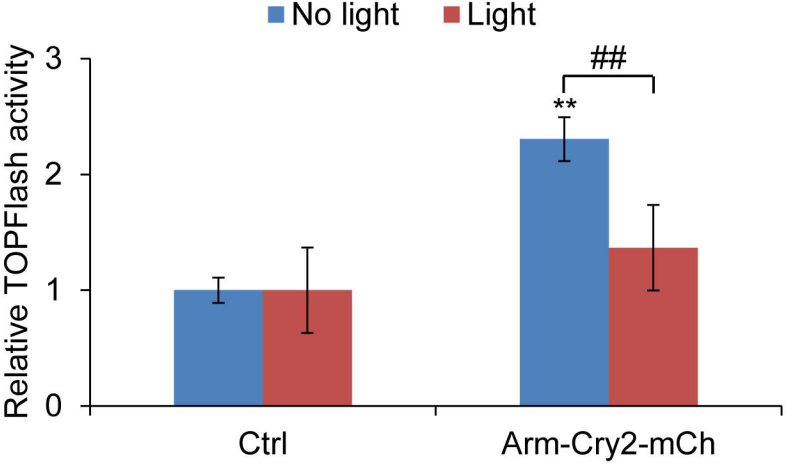
No light
Light
Relative TOPFlash activity
3
2
1
0
##
**
Ctrl
Arm-Cry2-mCh